

Adaptive control scheme for road profile estimation: application to vehicle dynamics[★]

M. Doumiati^{*} S. Erhart^{**} J. Martinez^{**} O. Sename^{**}
L. Dugard^{**}

^{*} *Heudiasyc Lab, Université de Technologie de Compiègne, 60200 Compiègne, France (email: moustapha.doumiati@hds.utc.fr).*
^{**} *Gipsa-Lab UMR CNRS 5216, Control Systems Department, Grenoble Institute of Technology ENSE3, BP 46, 38402 Saint Martin d'Hères, France (email: olivier.sename@gipsa-lab.grenoble-inp.fr).*

Abstract: Road profile is considered as an essential input that affects the vehicle dynamics. An accurate information of this data is fundamental for a better understanding of the vehicle behavior and vehicle control systems design. The present paper presents a novel algorithm (observer) suitable for real-time estimation of vertical road profile. The developed approach is based on a quarter-car model, and on elementary measurements delivered by potentially integrable sensors. The road elevation is modeled as a sinusoidal disturbance signal affecting the vehicle system. Since this signal has unknown and time-varying characteristics, the proposed estimation method implements an adaptive control scheme based on the internal model principle and on the use of the Youla-Kucera parametrization technique (also known as Q-parametrization). For performances assessment, estimations are comparatively evaluated with respect to measurements issued from the *LPA* (Longitudinal Profile Analyzer) profiler during experimental trials. Further, this new method is compared to the approach provided in (Doumiati et al. (2011)), where a Kalman filter is applied assuming a linear road model. Results show the validity and efficiency of the present observer scheme.

1. INTRODUCTION

Road geometries, irregularities and deformations constantly modify vehicle positions and wheel orientations. Road profile is considered as an essential input that affects the vehicle dynamics. The knowledge of this significant signal is essential for road quality evaluation, road roughness index calculation (see (Gillespie (1992)), and (Sayers and Karamihas (1998))), analysis of vehicle dynamics, suspensions design, and control systems development (see (Bastow et al. (2004)), (Elmadany and Abduljabbar (1999)), and (Savaresi et al. (2010))). Its on-board evaluation would significantly help to adjust the vehicle dynamics and suspension parameters to improve passengers safety, and ride comfort. However, nowadays, there is no low-cost sensor that directly measures the road elevation. This motivates the development of an observer, also known as virtual sensor, to reconstruct this data.

For the purpose of road survey and maintenance, several instruments (also called profilers) evaluating road quality were developed in research labs and industries. Profilers or profilometers are instruments and methods used to produce a sequence of numbers related to the true road profile. A profiler works by combining three main components: a reference elevation, a height relative to the reference, and the longitudinal distance (Sayers and Karamihas (1998)). These ingredients are combined in different ways, based on the design of the profiler. Among the different existing profilers, one could cite:

- The (*LPA*) device developed by the Roads and Bridges Central laboratory in France (IFSTTAR laboratory previously named LCPC): this system illustrated in Figure 1 includes one or two single wheel

trailers towed at constant speed by a car and a data acquisition system. A ballasted chassis supports an oscillating beam holding a feeler wheel that is kept in permanent contact with the pavement by a suspension and damping system. The chassis is connected to the towing vehicle by a joint. Vertical movements of the wheel result in angular travel of the oscillated beam, measured with respect to the horizontal arm of the inertial pendulum, independently of movements of the towing vehicle (Imine et al. (2006)).

- The inertial high speed profiler basically introduced by the General Motors research laboratory (Sprangler and Kelly (1964)): this technique uses accelerometers placed on the body of the measuring vehicle to establish an inertial reference. The recorded profile is obtained by calculating the relative displacement between the accelerometers and the pavement surface (see (Gillespie (1992)), (Imine et al. (2005)), and (Imine et al. (2006))).

The major drawback of the aforementioned profilers is their inapplicability in ordinary vehicles for technical and economical reasons.

Recently, Mercedes-Benz introduces in its new 2014 S- and E-Class cars stereo cameras for road profile scanning (Mercedes-Benz (2014)). Other existing approaches consist to estimate the road elevation using virtual sensors (observers). In (Imine et al. (2005)) and (Imine et al. (2006)), estimation techniques based on sliding mode observers were proposed. These model-based methods consider full car model of 16 Degree Of Freedom (DOF). Such a model appears time-consuming for real-time implementation. In (Doumiati et al. (2011)), authors propose a method based on a quarter-car model and Kalman filter for on-board estimation of road elevation. The studies in (Doumiati et al. (2011)), (Imine et al. (2005)) and (Imine et al.

[★] This work was supported by the national French project INOVE/ANR 2010 BLAN 0308 (www.gipsa-lab.fr/projet/inove).

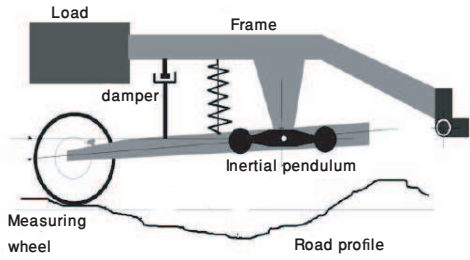


Fig. 1. *LPA*: Longitudinal Profile Analyzer (Imine et al. (2006)).

(2006)) assume linear road profile models, where the road accelerations are negligible. However, this hypothesis does not fully satisfy the analysis of the longitudinal road profile presented in (Sayers and Karamihas (1998)). Therein, a demonstration is given that even small road profile variations could lead to considerable road accelerations depending on the current vehicle velocity. According to the road roughness classification *ISO 8608* discussed in (Gonzales et al. (2008)), a real road profile could be interpreted and evaluated by means of its spectral decomposition. A typical road profile has no direct resemblance to a pure sinusoid, but it encompasses a spectrum of sinusoidal wave lengths. This hypothesis is adopted in this study, and constitutes one of its particularity with respect to others existing in literature. The proposed procedure considers the road profile as unpredictable input disturbance to the vehicle system. Since this disturbance has unknown and time-varying frequencies, the estimation problem is tackled in the context of the feedback adaptive control while applying the internal model principle (introducing the disturbance model into the controller) (refer to (Ioannou and Sun (1996)) and (Landau et al. (2011))). To simplify the design and reduce the computation load, the developed controller is built within the Youla-Kucera parametrization framework.

The rest of the paper is organized as follows. Section 2 describes the adopted vehicle and road models. Section 3 deals with the estimation process and discusses the observer design in a control scheme. Section 4 compares the estimation results to measured profiles from *LPA* during experimental tests. Finally, Section 5 provides concluding remarks and some perspectives for future works.

2. MODELS OF THE VEHICLE/ROAD INTERACTIONS

Suitable vehicle and road models must be assumed in order to implement a model-based observer. The adopted models will be discussed in the next.

2.1 Quarter-car vehicle model

For on-board implementation reason, a simple linear passive quarter-car vehicle model is considered. This model represents a corner of a vehicle as shown in Figure 2, and accounts for about 75% of the vertical vibrations present on a vehicle (Sayers and Karamihas (1998)). The suspension system joins chassis and tire. The sprung mass of the car body, m_s , is connected by a spring and damper to the unsprung mass of the suspension components, m_u , by the suspension spring, k_s , and the damper c_s . The tire is linked with the road displacement, $u(t)$, involving the tire stiffness, k_t . It is generally assumed that the tire damping is negligible. A study of analysis of k_s , c_s , k_u , k_t parameters on the suspension/tire performance is drawn in (Rajamani (2006)).

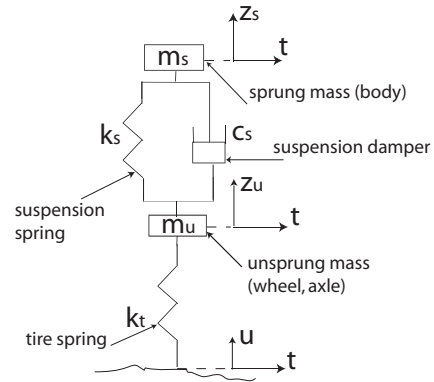


Fig. 2. Quarter-car vehicle model.

A straightforward driven situation is considered. Hence, suspension dynamics are especially due to the road inputs and not to roll/pitch motions. An analysis of the full car and half car models' response to road irregularities given in (Rajamani (2006)) indicated that the suspensions can be designed independently at each wheel. The quarter car suspension model is therefore adequate to study and design automotive suspension systems for optimizing response to road irregularities.

Assuming that wheels are rolling without slip and without contact loss, relations (1) and (2) represent the motion of the vehicle body and the wheel respectively:

$$m_s \ddot{z}_s = -k_s z_s - c_s \dot{z}_s + k_s z_u + c_s \dot{z}_u, \quad (1)$$

$$m_u \ddot{z}_u = -(k_s + k_t) z_u - c_s \dot{z}_u + k_s z_s + c_s \dot{z}_s + k_t u, \quad (2)$$

where $z_s(t)$ is the position of the vehicle body, $z_u(t)$ is the position of the wheel, and the *dot* denotes the time derivative, i.e., $\dot{z}_s = \frac{d^2 z_s}{dt^2}$. In the *Laplace-domain*, the transfer function between the road profile $U(s)$ and the chassis position $Z_s(s)$, known as the road-to-body transmissibility equation, is of fourth-order and can be given by (3):

$$\frac{Z_s(s)}{U(s)} = \frac{a_1}{b_1 \cdot b_2 - b_3}, \quad (3)$$

where: $a_1 = k_t (sc_s + k_s)$, $b_1 = (s^2 m_s + sc_s + k_s)$, $b_2 = (s^2 m_u + sc_s + k_s + k_t)$, $b_3 = (sc_s + k_s)^2$.

2.2 Road profile model

As the vehicle moves over the road profile at a speed v , the static spatial waves (irregularities) of the road are transformed into a *time-variant* sinusoid elevation at the wheel, $u(t)$. The relation between the spatial wavelength, λ (respectively the wave number $\gamma = \frac{1}{\lambda}$) imposed by a road profile and the resulting oscillation frequency, f , of the elevation signal is given by (Sayers and Karamihas (1998)):

$$f = \frac{v}{\lambda} = v \cdot \gamma. \quad (4)$$

It could be observed that the travel speed affects how vehicle sees sinusoids in the road. In reality, a typical road profile is a stochastic signal that has no direct resemblance to a pure sinusoid, but considered as a composition of series of sinusoidal waves (see (Rajamani (2006)), and (Sayers and Karamihas (1998))). Figure 3 shows an example of spectrum of two different real road profiles collected

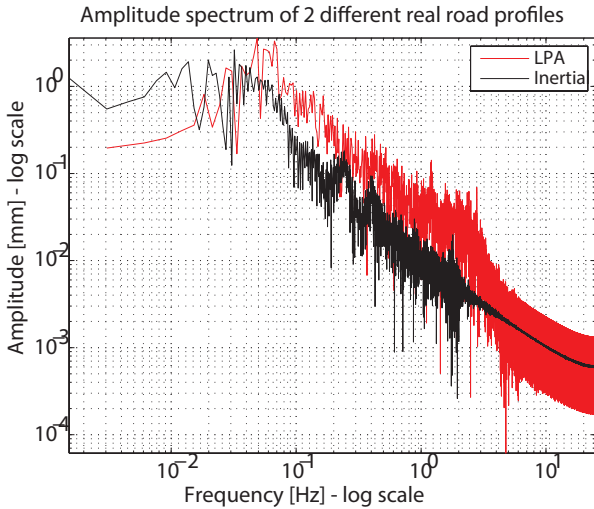


Fig. 3. An example of spectrum of two real road profiles.

through *LPA* and inertial profilers. These measurements are obtained using two laboratory cars moving at 75 *Km/h* and 20 *Km/h* respectively. The spectrum of these low-pass signals are computed using the Fast Fourier transform.

Working hypothesis: In this study, thereafter, it is assumed that the time-based dynamics of the road profile can be modeled as a finite series of N sinusoids with different wavelengths, λ_i , frequencies, f_i , amplitudes, C_i , and phases, ϕ_i :

$$u(t) = \sum_{i=1}^N C_i \sin(2\pi f_i t + \phi_i). \quad (5)$$

Note that C_i , f_i , and ϕ_i are unknown time-varying parameters. The objective of this paper is not to evaluate these parameters separately, but to estimate the road elevation $u(t)$.

3. OBSERVER DESIGN

3.1 Problem formulation

The estimation process developed in this study is formulated as a closed-loop regulation approach, trying to attenuate the difference e between the measured chassis position, z_s and the estimated quarter-car model output \hat{z}_s (see Figure 4). The chassis position signal is the result of the real profile u , exciting the vehicle system. A linear relation is assumed between z_s and u . The signal u is considered as a time-varying sinusoidal disturbance. When the estimated chassis position coincides with the corresponding measured one, so will also the estimated profile \hat{u} be equivalent to u . In other terms, the command, \hat{u} , could be interpreted as the estimated road profile required to produce \hat{z}_s , so that $e = z_s - \hat{z}_s = 0$. The problem becomes to find a control law for unknown time-varying disturbances rejection, case where the plant model (vehicle system) is known, and the disturbance model (road) is of unknown parameters.

One of the approaches considered for solving this problem is to build/estimate the disturbance model, and then recompute the controller in real-time. This will lead to indirect adaptive control (Landau and Airimitoiaie (2013)). The time-consuming part of this approach is the redesign of the controller at each sampling time. This method seems not to be practical for the present application due to the

fast dynamics of the unpredicted variations of the road profile. Another way, known as direct adaptive control, consists to apply Youla-kucera parametrization of the controller also known as Q -parametrization, where it is possible to insert and adjust the internal model (model of the disturbance) in the controller by adjusting the parameters of the Q -polynomial without recomputing the whole controller (polynomials R_0 and S_0 remain unchanged, see Figure 5). Note that authors in (Constantinescu et al. (2007)) and (Landau and Airimitoiaie (2013)) proved that the direct adaptive control scheme has simpler structure, implementation, and provides better performance than an indirect adaptive control scheme, especially during transient dynamic phases. Based on the analysis given above, it is recommended to develop the road profile observer in the direct adaptive control framework.

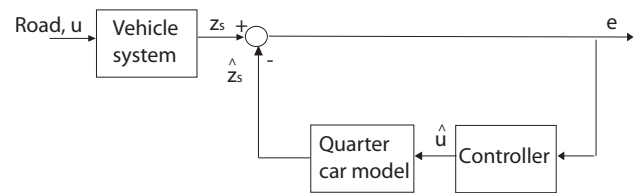


Fig. 4. Block diagram of the observer interpreted as a closed-loop control system.

3.2 Direct adaptive control Scheme

The discrete direct adaptive control scheme for time-varying disturbance rejection could be illustrated as in Figure 5. It uses Youla-kucera parametrization for the computation of the controller. This algorithm takes its root from the idea of Tsytkin (Tsytkin (1991)). In this case, the common framework is the assumption that the disturbance is the result of a white noise or a Dirac impulse passed through the "model of disturbance (road)" considered unknown. The polynomials $A(z^{-1})$ and $B(z^{-1})$ obtained using the Z-transform of Equation (3), represent the denominator and the numerator of the dynamic car model.

The adaptive controller to be built is of RS-type. Its dynamic is separated into a nominal part, defined by $[R_0(z^{-1}), S_0(z^{-1})]$, and a performing part given by the polynomial \hat{Q} that includes the disturbance model (\hat{Q} is the estimation of the Q polynomial requires to suppress disturbances). The controller $[R_0(z^{-1}), S_0(z^{-1})]$ is built so that it stabilizes the closed-loop system, and verifies desired specifications in the absence of the disturbance (without internal model of the disturbance, $\hat{Q} = 0$). It can be computed using classical methods in control theory. Once calculated, (R_0, S_0) remains unchanged in the control scheme, but \hat{Q} is adjusted according to an adaptive algorithm to make $e(t) = 0$ in presence of disturbance without modifying the closed-loop poles (Landau et al. (2005)). The order n_Q of the polynomial Q is fixed, and depends upon the structure of the disturbance model. It is seen that the Q -parametrization offers a supplementary degree of freedom into the controller permitting to treat separately the problem of disturbance suppression. For details, robustness and stability analysis of the Youla-Kucera parametrization in the framework of adaptive control, one can refer to (Ioannou and Sun (1996)), (Landau et al. (2005)), and (Landau et al. (2011)). This study is only restricted to a brief presentation of the adaptive algorithm, and the estimation of the polynomial \hat{Q} .

Let q^{-1} be the delay operator used for describing the

system behavior in the time domain (i.e $x(t) = q^{-1}x(t+1)$). Note that z^{-1} is used to describe the system behavior in the frequency domain, while q^{-1} represents its characteristics in the time domain. Using the Q -parametrization,

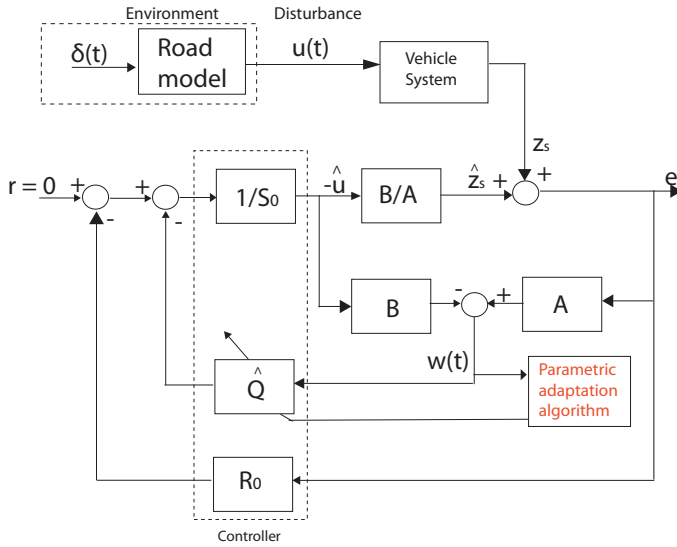


Fig. 5. Block diagram of the adaptive observer using the Q -parameterization.

the output of the system in the presence of disturbance can be written as:

$$e(t) = \frac{S_0(q^{-1}) - B(q^{-1})Q(q^{-1})}{P(q^{-1})}w(t), \quad (6)$$

where $P(q^{-1})$ represents the poles of the closed loop:

$$P(q^{-1}) = A(q^{-1})S_0(q^{-1}) + B(q^{-1})R_0(q^{-1}), \quad (7)$$

and $w(t)$ (see Figure 5) is:

$$w(t) = A(q^{-1})e(t) + B(q^{-1})\hat{u}(t). \quad (8)$$

In the time domain, the internal model principle could be explained as find Q such that $e(t)$ becomes zero asymptotically.

Define $\hat{Q}(t, q^{-1})$ the estimation of the polynomial Q at instant t :

$$\hat{Q}(t, q^{-1}) = \hat{q}_0(t) + \hat{q}_1(t)q^{-1} + \dots + \hat{q}_{n_Q}(t)q^{-n_Q}, \quad (9)$$

the associated estimated parameter vector:

$$\hat{\theta}(t) = [\hat{q}_0(t) \ \hat{q}_1(t) \ \dots \ \hat{q}_{n_Q}(t)]^T. \quad (10)$$

Define the following observation (regressor) vector:

$$\phi^T(t) = [w_2(t) \ w_2(t-1) \ \dots \ w_2(t-n_Q)], \quad (11)$$

where:

$$w_2(t) = \frac{B^*(q^{-1})}{P(q^{-1})}w(t), \quad B = q^{-1}B^*. \quad (12)$$

The *a priori* adaptation error, defined as the value of $e(t)$ obtained with $\hat{Q}(t, q^{-1})$, may be written as (details are provided in (Landau et al. (2009)), and (Landau et al. (2011))):

$$\epsilon^0(t+1) = w_1(t+1) - \hat{\theta}^T(t)\phi(t), \quad (13)$$

The *a posteriori* adaptation error (using $\hat{Q}(t+1, q^{-1})$), may be expressed as:

$$\epsilon(t+1) = w_1(t+1) - \hat{\theta}^T(t+1)\phi(t), \quad (14)$$

with

$$w_1(t+1) = \frac{S_0(q^{-1})}{P(q^{-1})}w(t+1), \quad (15)$$

$$w(t+1) = A(q^{-1})e(t+1) + B^*(q^{-1})\hat{u}(t), \quad (16)$$

where $B^*(q^{-1})\hat{u}(t) = B(q^{-1})\hat{u}(t+1)$.

For estimation of $\hat{Q}(t, q^{-1})$ parameters, the following Parameter Adaptation Algorithm (PAA) is used (Landau et al. (2005)):

$$\hat{\theta}(t+1) = \hat{\theta}(t) + F(t)\phi(t)\epsilon(t+1), \quad (17)$$

$$\epsilon(t+1) = \frac{\epsilon^0(t+1)}{1 + \phi^T(t)F(t)\phi(t)}, \quad (18)$$

$$\epsilon^0(t+1) = w_1(t+1) - \hat{\theta}^T(t)\phi(t), \quad (19)$$

$$F(t+1) = \frac{1}{\lambda_1(t)}\left(F(t) - \frac{F(t)\phi(t)\phi^T(t)F(t)}{\alpha(t) + \phi^T(t)F(t)\phi(t)}\right), \quad (20)$$

where $F(t)$ is a time-varying adaptation gain (positive definite matrix), and $\alpha(t) = \frac{\lambda_1(t)}{\lambda_2(t)}$. $F(t)$ can be interpreted as a measure of the parametric error. The tuning factors $\lambda_1(t)$ and $\lambda_2(t)$ permit the adjustment of the adaptation speed. An adaptation gain with a variable forgetting factor, $\lambda_1(t)$ combined with a constant trace of $F(t)$ is chosen here to track automatically the changes of road characteristics (Landau et al. (2005)).

For *adaptive* operation, the following procedure works continuously and is applied sequentially at each sampling time:

- (1) Get $e(t+1)$ and $-\hat{u}(t)$ to compute $w(t+1)$ using (16).
- (2) Compute $w_1(t+1)$ and $w_2(t)$ through (12) to (15).
- (3) Estimate the Q -polynomial using the parametric adaptation algorithm given by (17) to (20)
- (4) Calculate $\hat{u}(t+1)$ according to:

$$S_0(q^{-1})\hat{u}(t+1) = R_0(q^{-1})e(t+1) + \hat{Q}(t, q^{-1})w(t+1). \quad (21)$$

4. EXPERIMENTAL RESULTS

In this section, the estimated road profile is compared to the measured one coming from *LPA* in order to test its validity (the *LPA* device of the LCPC lab was briefly described in the Introduction). The signal measured by the *LPA* constitutes our reference profile. Data were collected during real trials, and then treated off-line. In the following, the test description, observer configuration and results are illustrated and analyzed. A comparison of the present methodology with the approach developed in (Doumiati et al. (2011)) is also provided in the next.

4.1 Test description

The experimental vehicle shown in Figure 6 is the LCPC Laboratory's test vehicle. It is a Peugeot 406 equipped with accelerometers, relative suspension deflections sensor and towing *LPA* for road profile measurement. The suspension/tire parameters are: $m_s = 378 \text{ Kg}$, $c_s = 3000 \text{ Ns/m}$, $k_s = 21319 \text{ N/m}$, $m_u = 36.8 \text{ Kg}$, and $k_t = 100000 \text{ N/m}$ (Imine et al. (2006)). Among numerous experimental tests, a trial made at the LCPC Laboratory test track is considered. The car runs on an irregular surface with a quasi-constant speed of 72 km/h along 600 m . The results illustrated in the following correspond to the left front wheel. Figure 3 shows the spectrum of the collected road profile (see the *LPA* measurement). Figure 7 shows the body position influenced by the road input at the wheel. This signal is obtained by a double integration of the signal generated by the accelerometer sensor installed at the vehicle corner in the vertical direction (Doumiati et al. (2011) and Doumiati et al. (2013)).



Fig. 6. LCPC laboratory vehicle towing *LPA* (Imine et al. (2006)).

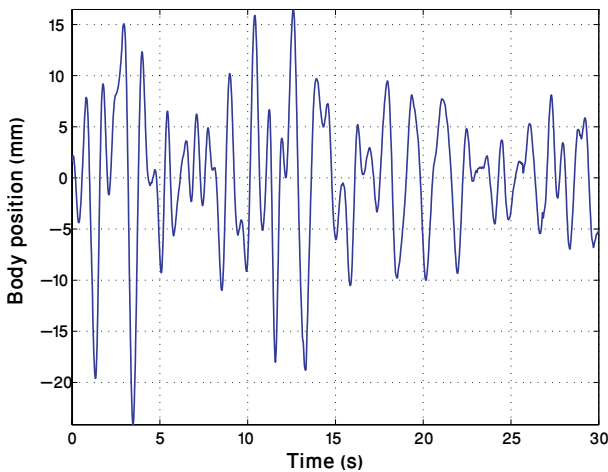


Fig. 7. Up and downward vehicle body movement due to road irregularities.

4.2 Configuration of the controller

Based on some results obtained for different trials tested off-line, the number of coefficients of \hat{Q} is heuristically selected to be $n_Q = 6$. These coefficients are initialized with 0. Regarding the nominal controller (R_0, S_0) (without the internal model of the disturbance), it is designed via *MATLAB/SISO* tool so that it reconstructs the low frequencies part of the profile elevation. Figure 8 draws the output sensitivity function of the system defined as the transfer function between z_s and the output of the system, e :

$$\frac{e}{z_s} = \frac{S_0 A}{S_0 A + R_0 B}, \text{ where } \hat{Q} = 0. \quad (22)$$

The polynomials $R_0(z^{-1})$ and $S_0(z^{-1})$ are found to be:

$$R_0 = 9.15 - 16.6z^{-1} + 8.04z^{-2}, \quad S_0 = 1 - z^{-1} \quad (23)$$

4.3 Observer validation and comparison with *LPA* and (Doumiati et al. (2011))

Figure 9 plots the estimated longitudinal road profile via the proposed control approach, and the one measured by the *LPA*. Clearly, the estimated values match well the *LPA* signal. However, some discrepancies in amplitudes persist. They might be caused by sensors calibration and signals filtration process in the *LPA* system. Figure 10 shows the variations of the polynomial \hat{Q} coefficients. These coefficients are adapted as function of the involved

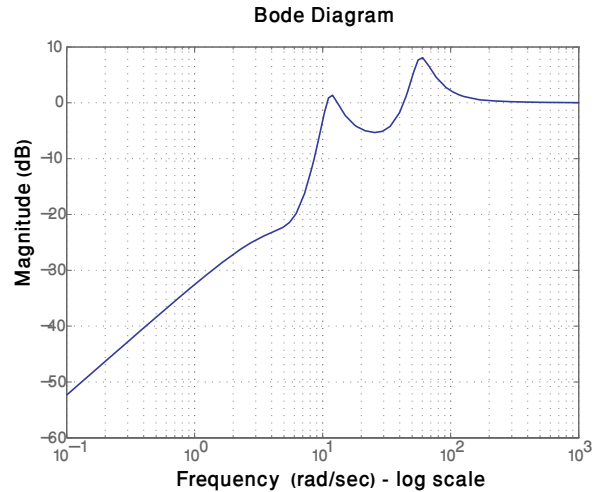


Fig. 8. Output sensitivity function.

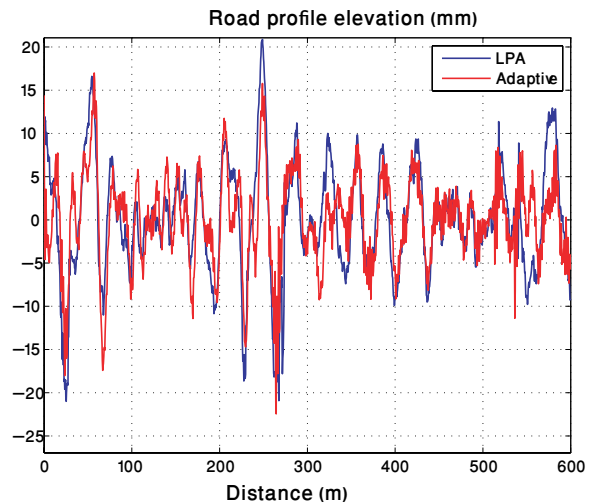


Fig. 9. Comparison between the proposed adaptive observer approach and the *LPA* profiles.

road frequencies, and converge to some suitable values minimizing the output, e .

For a more precise quantification of the estimation quality, Figure 11 illustrates the spectrum of the estimation error, $u - \hat{u}$. The observer performs well especially for low frequencies corresponding to high wavelengths. This figure also compares the performance of the present method to the study given in (Doumiati et al. (2011)). Recall that this previous study assumes low acceleration signal (related to the road), $\ddot{u} = 0$, and applies a model-based stochastic Kalman filter to estimate the profile elevation. The novel approach points out better results especially for small frequencies which is crucial for suspension control. This is mainly due to the better representation/modeling of the road profile in the estimation process. It is also worth noting that the present algorithm is less costly than the one given in (Doumiati et al. (2011)), since it requires only information regarding the body position, while the previous method needs both measurements of the suspension deflections and the body position.

5. CONCLUSION

This paper described a new model-based estimation process suitable for real-time implementation to reconstruct

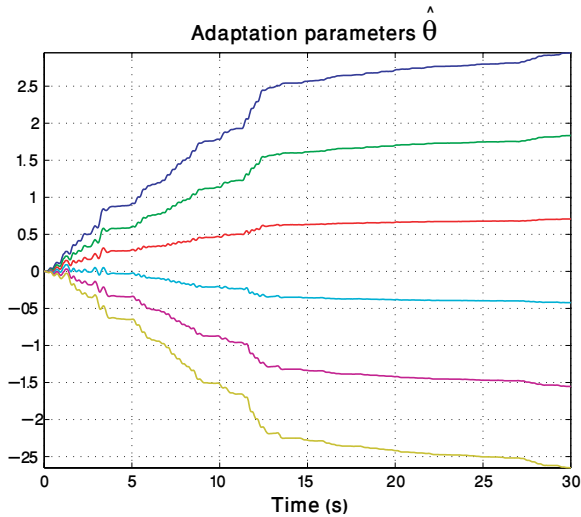


Fig. 10. Evolution of \hat{Q} parameters during adaptation.

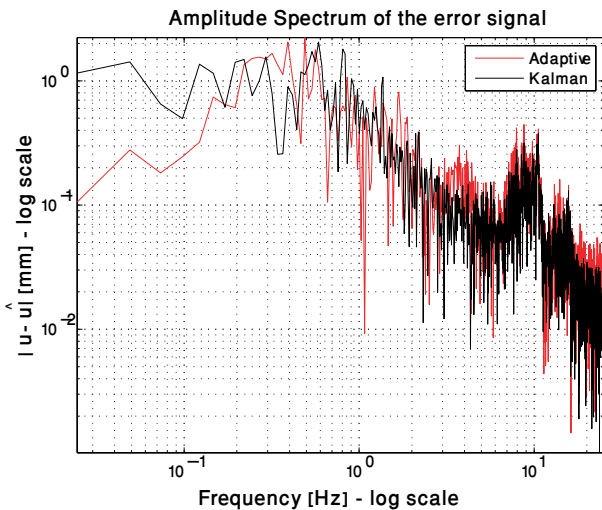


Fig. 11. Spectrum of the estimation error signal, $u - \hat{u}$: comparison between the proposed adaptive approach and the observer given in (Doumiati et al. (2011)).

longitudinal road profile. The vehicle was represented by a quarter-car model while the road surface was modeled by a finite number of sinusoids with time-varying characteristics. Since the estimation quality strongly depended on the choice of the considered frequencies for the profile representation, an adaptive Q-parametrized observer scheme was designed and applied. The road profile observation problem tackled in an adaptive control scheme can be considered as a major contribution of this research. The profile reconstruction capacity was successfully tested by means of numerical simulations using experimental data issued from the LPA profiler. Results confirmed the validity of the postulated working hypothesis.

Further investigations consist to apply half or full-car vehicle model instead of a simple quarter-car model for a better representation of the vehicle dynamics in different driving situations (cornering, steering, accelerating, and braking). The proposed method will be also applied to the INOVE testbed for validation (www.gipsa-lab.fr/projet/inove).

ACKNOWLEDGEMENTS

Special thanks to the LCPC (www.ifttar.fr) for the experimental data collected through their LPA. This real data was delivered in the framework of SARI/RADARR project in collaboration with Heudiasyc laboratory, France (www.hds.utc.fr).

REFERENCES

- D. Bastow, G. Howard, and J. P. Whitehead. *Car suspension and handling*. SAE International, 2004.
- A. Constantinescu, D. Rey, and I.D. Landau. Rejection of narrow band unknown disturbances in an active suspension system. In *Proceedings of the European Control Conference, Kos, Greece, 2007*.
- M. Doumiati, A. Victorino, A. Charara, and D. Lechner. Estimation of road profile for vehicle dynamics motion: experimental validation. In *Proceedings of the American Control Conference, St Francisco, CA, USA*, pages 5237–5242, 2011.
- M. Doumiati, A. Charara, A. Victorino, and D. Lechner. *Vehicle dynamics estimation using Kalman filtering - Experimental validation*. ISTE ltd and J. Wiley, 2013.
- M. M. Elmadany and Z. S. Abduljabbar. Linear quadratic gaussian control of a quarter-car suspension. *Vehicle System Dynamics*, 32:479–497, 1999.
- T. D. Gillespie. *Fundamentals of vehicle dynamics*. Society of Automotive Engineers, 1992.
- A. Gonzales, E.J. O'Brien, Y.Y. Li, and K. Cashell. The use of vehicle acceleration measurements to estimate road roughness. *Vehicle System Dynamics*, 46:483–499, 2008.
- H. Imine, Y. Delanne, and N.K. M'sirdi. Road profile inputs for evaluation of the loads on the wheels. *Vehicle System Dynamics*, Supplement 43:359–369, 2005.
- H. Imine, Y. Delanne, and N.K. M'sirdi. Road profile input estimation in vehicle dynamics simulation. *Vehicle System Dynamics*, 44(4):285–303, 2006.
- P. A. Ioannou and J. Sun. *Robust adaptive control*. Prentice-Hall, 1996.
- I. Landau, A. Constantinescu, and D. Rey. Adaptive narrow band disturbance rejection applied to an active suspension—an internal model principle approach. *Automatica*, 41:563–574, 2005.
- I.D. Landau and T. Airimitoai. An indirect adaptive feedback attenuation strategy for active vibration control. In *Proceedings of the 21st Mediterranean Conference on Control and Automation, Chania, Greece, 2013*.
- I.D. Landau, A. Constantinescu, and M. Alma. Adaptive regulation - rejection of unknown multiple narrow band disturbances. In *Proceedings of the 17th Mediterranean Conference on Control and Automation, Thessaloniki, Greece, 2009*.
- I.D. Landau, R. Lozano, M. M'Saad, and A. Karimi. *Adaptive control: Algorithms, Analysis and Applications*. Springer-Verlag, 2011.
- Mercedes-Benz, 2014. URL <http://www5.mercedes-benz.com>.
- R. Rajamani. *Vehicle dynamics and control*. Springer, 2006.
- S. M. Savaresi, C. Poussot-vassal, C. Spelta, O. Sename, and L. Dugard. *Semi-active suspension control design for vehicles*. Elsevier, Butterworth Heinemann, 2010.
- M. W. Sayers and S. M. Karamihas. *The little book of profiling*. University of Michigan, 1998.
- E.B. Sprangler and W.J. Kelly. *Profilometer method for measuring road profile*. General Motors Research Publication GMR-452, 1964.
- Y. Tsyphkin. *Adaptive invariant discrete control systems*. Springer Verlag, 1991.